

Published in IET Science, Measurement and Technology
 Received on 4th June 2008
 Revised on 20th August 2008
 doi: 10.1049/iet-smt:20080088

Special Issue – selected papers from CEM 2008



Extraction from field models of the lumped parameters of induction motors

F. Henrotte J. Heidt E. Lange M. van der Giet K. Hameyer

*Institute for Electrical Machines, RWTH Aachen University, Schinkelstraße 4, Aachen 52056, Germany
 E-mail: fh@iem.rwth-aachen.de*

Abstract: Mathematical background for the definition of the lumped parameters of the equivalent T-diagram of induction motors is described. It is shown how one can systematically extract the lumped parameters from a number of finite element transient simulations.

1 Introduction

The equivalent T-circuit of an induction machine is a very useful and widely used representation found in every engineering book. It is also becoming increasingly important with the development of vector control, as the values calculated with the equivalent circuit are used in the control process of the Pulse-width modulation (PWM) inverter. The T-diagram is, thus, the bridge between the finite element representation of the motor and the motor controller [1].

A glance into the literature on the subject shows that the lumped parameters of the equivalent T-circuit are usually determined empirically, for example [2–7], or on the basis of an energy analysis [1]. Clearly, there exist several definitions usually stated without a justification, and a compelling theoretical framework is still lacking.

Basic principles and mathematical background of the lumped parameter identification methods in the case of an induction motor are discussed in this paper. The idea is to provide a general definition for lumped parameters in the equivalent T-circuit. This approach enables drawing some interesting conclusions about the domain of application and the accuracy of the T-circuit representation of electrical machines.

2 Principle

The definition of the equivalent T-circuit of an induction machine is a simplification, whose validity relies on the fact

that the induction field exhibits a well-defined and permanent geometrical structure when the machine is operated in steady state. There is not much quantitative information to retrieve from the general appearance of the vector potential plot in an electrical machine, which always look the same (Fig. 1). On the contrary, this regularity is precisely the redundancy one attempts to get rid of by defining the equivalent T-circuit.

The notion of lumped parameters stems from the existence of a relation between the local variables, which are the electromagnetic fields (magnetic vector potential \mathbf{a} , current density \mathbf{j} and electric scalar potential u), and the associated global quantities describing the system (flux linkages ϕ_r , electric currents I_r and voltages ΔU_r). Global quantities are also called integral variables or phase variables, and they are directly linked with the measurable quantities of the machine (voltages, currents). See [8] and the references therein for a detailed theoretical introduction. The next section shows how one can systematically draw the link between the local and global quantities.

3 Lumped parameter extraction

3.1 Energy balance in magnetodynamics

The lumped parameters that represent an electrical machine seen from its stator terminals are the phase voltages ΔU_r , the phase resistances R_r , the inductance matrix L_{rs} and the electromotive forces E_r induced in stator windings by the rotation of the machine, in which $r = 1, \dots, m$, where

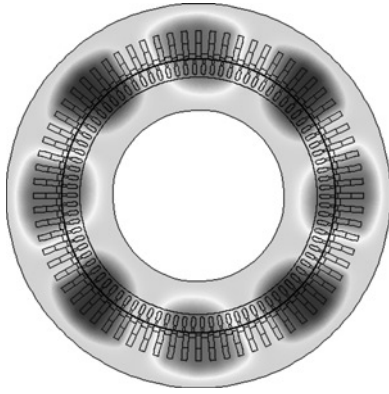


Figure 1 Vector potential in an induction motor in rated conditions

$m = 3$ is the number of phases. One has

$$\Delta U_r = R_r I_r + \partial_t \phi_r \quad (1)$$

$$= R_r I_r + (E_r + L_{rs} \partial_t I_s) \quad (2)$$

where ϕ_r is the flux linkage in phase r .

A relation between the local state variable (the vector potential \mathbf{a}) and the global state variables (the phase fluxes ϕ_r) is obtained on the basis of energy considerations. Multiplying (1) with I_r and summing over all phases gives

$$\sum_r I_r \partial_t \phi_r = - \sum_r R_r I_r^2 + \sum_r I_r \Delta U_r \quad (3)$$

This equation has a counterpart in the field domain [9]

$$\int_{\Omega} \mathbf{j} \cdot \mathcal{L}_v \mathbf{a} = - \int_{\Omega} \frac{j^2}{\sigma} - \int_{\Omega} \mathbf{j} \cdot \text{grad } u \quad (4)$$

where $\mathcal{L}_v \mathbf{a}$ denotes the material derivative of \mathbf{a} , that is, a time derivative accounting for movement. Equations (4) and (3) must be identifiable term by term to ensure that the energy balance in the field domain and in the lumped parameter domain are equivalent.

The current density \mathbf{j} is now expressed in terms of the currents I_r flowing in the system

$$\mathbf{j} = \sum_r I_r \mathbf{w}_r \quad (5)$$

where the auxiliary field \mathbf{w}_r can be regarded as the shape functions of the phase currents I_r . Substituting (5) in (4) yields definitions for the phase resistances and the phase voltages

$$R_r = \int_{\Omega} \sigma^{-1} |\mathbf{w}_r|^2, \quad \Delta U_r = - \int_{\Omega} \mathbf{w}_r \cdot \text{grad } u \quad (6)$$

On the other hand, substituting (5) in

$$\int_{\Omega} \mathbf{j} \cdot \mathcal{L}_v \mathbf{a} = \sum_r I_r \partial_t \phi_r \quad (7)$$

yields a definition for the time derivative of the flux linkage

$$\partial_t \phi_r = \int_{\Omega} \mathbf{w}_r \cdot \mathcal{L}_v \mathbf{a} \quad (8)$$

If the current distribution functions \mathbf{w}_r are assumed not to depend on time (which is the case in stranded coils), the time derivatives can be dropped, and the mapping sought between \mathbf{a} and ϕ_r is

$$\phi_r = \int_{\Omega} \mathbf{w}_r \cdot \mathbf{a} \quad (9)$$

3.2 Discussion

The previous section has provided a theoretical discussion of the definition (9), which is commonly found in the literature. In systems with several coils, the relation between fluxes and currents is usually represented under matrix form as

$$\phi_r = \sum_s L_{rs} I_s \quad (10)$$

where L_{rs} is the inductance matrix of the system. Equation (9), however, does not allow making the separation between the contribution to the flux ϕ_r of the current I_r flowing in the coil under consideration, and the contributions of other currents flowing in other coils of the system. The individual components of the inductance matrix must therefore be determined by inspection, that is, by supplying the coils individually one after the other, identifying each time one column of the inductance matrix in this manner. This indicates that the superposition principle is applied, whereas magnetic cores in electrical machines have nonlinear magnetic behaviour in general.

There are a number of additional difficulties associated with this method of defining the inductance matrix:

- Equation (9) does not provide a definition for the fluxes that are not associated with a coil, for example for leakage fluxes or air gap fluxes.
- It cannot be adapted in a straightforward manner to define fluxes in massive conductors (e.g. squirrel cage rotor) where the current shape function \mathbf{w}_r is not known a priori.
- It is unclear, in the nonlinear case, in which manner the components L_{rs} should depend on the different currents I_r (or the fluxes ϕ_r).

This is the reason why most definitions of equivalent circuit diagrams are rather empirical or pragmatic. If this works fine, for example, with transformers [10, 11], the extension to an

induction motor is not trivial, essentially because of motion and skin effects in the squirrel cage bars. The above questions must indeed be answered if one wants to obtain a rigorous definition of an inductance matrix in general, and of the equivalent circuit of an induction motor in particular.

4 Fields and their integral quantities

For this purpose, specific notions are introduced first. From a theoretical point of view, the induction field b can advantageously be regarded as a map that associates a real number, the flux φ , to any smooth surface Σ in the system

$$b : \Sigma \mapsto \varphi = \int_{\Sigma} b \in \mathbb{R} \quad (11)$$

This map has the natural linear property

$$\int_{\Sigma_1 + \Sigma_2} b = \int_{\Sigma_1} b + \int_{\Sigma_2} b \quad (12)$$

where Σ_1 and Σ_2 are two arbitrary smooth surfaces. It is called a differential form of degree 2 in mathematical language. The vector field b is then a practical representation of that map. One has the equivalence

$$\int_{\Sigma} b \equiv \int_{\Sigma} b \cdot n \, d\Sigma \quad (13)$$

where n is the unit normal vector to the surface Σ .

On the other hand, the vector potential a can be regarded as a map that associates a real number to any smooth curve Γ in the system

$$a : \Gamma \mapsto \varphi = \int_{\Gamma} a \in \mathbb{R} \quad (14)$$

It is called a differential form of degree 1 and it can also be represented by a vector field a . One has the equivalence

$$\int_{\Gamma} a \equiv \int_{\Gamma} a \cdot t \, d\Gamma \quad (15)$$

where t is the unit tangent vector to the curve Γ . Since $b = \text{curl } a$, by application of Stokes' theorem, one has a second definition for the flux through Σ

$$\varphi = \int_{\Sigma} b \cdot n \, d\Sigma = \int_{\Sigma} \text{curl } a \cdot n \, d\Sigma = \int_{\partial\Sigma} a \cdot t \, d\partial\Sigma \quad (16)$$

where ∂ is the boundary operator.

Comparing (16) with (9), one sees that the integration is not done here over a volume, but over a closed curve. Therefore for the sake of clarity, we have adopted different

names and notations. The mathematical flux φ_k should be carefully distinguished from the flux embraced by a coil ϕ_k , which is obtained by integration over the volume of an idealised stranded current density.

The magnetic field b and the current density j are also differential forms. As a differential form of degree 1, the magnetic field is evaluated on curves and the value is called the magnetomotive force

$$f = \int_{\Gamma} b = \int_{\Gamma} b \cdot t \, d\Gamma \quad (17)$$

On the other hand, the current density is a differential form of degree 2. It is evaluated on surfaces and the value is the current flowing through Σ

$$i = \int_{\Sigma} j = \int_{\Sigma} j \cdot n \, d\Sigma \quad (18)$$

They can also both be represented by vector fields, which then obey Ampere's law

$$\text{curl } b = j \quad (19)$$

It follows

$$i = \int_{\Sigma} j \cdot n \, d\Sigma = \int_{\partial\Sigma} b \cdot t \, d\partial\Sigma \quad (20)$$

The correspondences between local and global quantities in electrodynamic systems are summarised in Table 1.

5 Skeleton of a and the co-skeleton

As mentioned above, the vector potential field in an induction machine in steady-state operation exhibits a well-defined and permanent geometrical structure where the different poles and the air gap are clearly visible. In other words, all vector potential plots look more or less the same and this regularity is precisely the redundancy, the useless information, one attempts to get rid of by defining the equivalent circuit.

Table 1 Relation between local and global quantities in electrodynamic problems

	Local/Field	Integral/Measurable
coils	a	ϕ_k
	u	U_k
	j	I_k
skeleton	a	φ_k
co-skeleton	h	f_k
	j	i_k

As the vector potential evaluates on closed curves, the first step is to select the characteristic curves of the \mathbf{a} field, that is, a small set of closed curves, whose associated fluxes give the most information about the field. Because of the symmetry, one can restrict the analysis to one pole pair of the machine. One defines the following characteristic curves:

- C_1 : A closed curve located in the stator domain that embraces the maximal flux. This flux is noted as φ_1 . The closed curve C_1 should appear as a couple of points in a 2D representation. For clarity, it is represented in Fig. 2 by a surface Σ_1 such that $C_1 = \partial\Sigma_1$. Note that this surface is not unique, although the flux is well defined.
- C_2 : A closed curve located in the squirrel cage domain that embraces the maximal flux. This flux is noted φ_2 . C_2 is represented in Fig. 2 by a surface Σ_2 such that $C_2 = \partial\Sigma_2$.
- C : A closed curve located in the air gap that embraces the maximal flux. This flux is noted φ . C is represented in Fig. 2 by a surface Σ such that $C = \partial\Sigma$.

These three curves define a topological structure with the form of a double cylinder (Fig. 3), which can be regarded as the skeleton of the \mathbf{a} field. Besides the surfaces Σ_1, Σ_2 and Σ defined above, two additional cylindrical surfaces are needed to close the skeleton. The surface $\Sigma_{1\sigma}$ is such that $\partial\Sigma_{1\sigma} = C - C_1$ and the surface $\Sigma_{2\sigma}$ is such that $\partial\Sigma_{2\sigma} = C_2 - C$. They are associated, respectively, with the leakage fluxes $\varphi_{1\sigma}$ and $\varphi_{2\sigma}$, and they appear as two segments in Fig. 2. Note that the skeleton follows the rotating field, that is, it rotates at the speed $\omega_0 = 2\pi f_0/p$, where f_0 is the frequency and p the number of pole pairs.

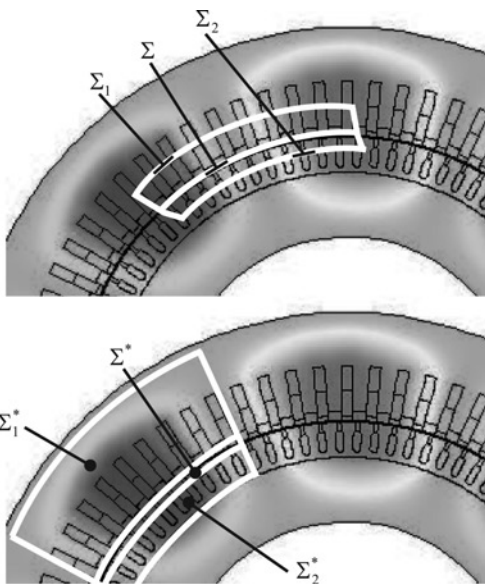


Figure 2 Zoom-in on one pole pair of a typical 2D vector potential plot in an induction machine, with the skeleton (above, surfaces Σ 's perpendicular to the plane) and the co-skeleton (below, surfaces Σ^* 's in plane)

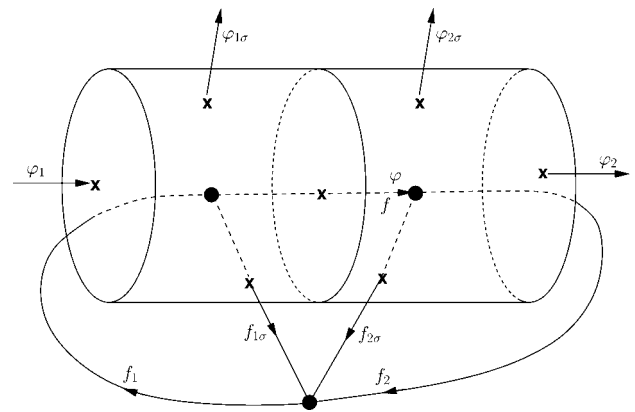


Figure 3 Skeleton (double cylinder) and co-skeleton (pretzel) with representation of the characteristic fluxes φ_k and magnetomotive forces f_k

By Poincaré duality, the skeleton can be associated with a dual topological structure called co-skeleton, which has the shape of a pretzel in this particular case, Fig. 3. Each element of dimension p of the skeleton is associated with an element of dimension $3 - p$ of the co-skeleton, (Table 2). Since the skeleton has no points (it is made out of closed curves only), the co-skeleton has no volume and is a flat surface. To each skeleton volume corresponds a co-skeleton point, that is, one point inside each cylinder plus a third point for the exterior.

One has, thus, the following characteristic surfaces:

- Σ_1^* : Surface located in the stator plane, which embraces the maximal current. This current is noted i_1 .
- Σ_2^* : Surface located in the rotor plane, which embraces the maximal current. This current is noted i_2 .
- Σ : Surface of the air gap. Note that the external node of the co-skeleton is any point on the left flank of the

Table 2 Number of topological elements of different dimensions in the skeleton and the co-skeleton of an induction machine

	Dimension	Skeleton	Co-skeleton
points	0	0	3
curves	1	3 (C)	5 (C^*)
surfaces	2	5 (Σ)	3 (Σ^*)
volumes	3	3	0

By Poincaré duality, the number of elements of dimension p in the skeleton is equal to the number of elements of dimension $3 - p$ in the co-skeleton. Between parenthesis are the symbols used in this paper

co-skeleton, since the tangential component of \mathbf{b} is zero on that curve, that is, all circulations vanish.

In particular, the co-skeleton surfaces dual to C_1 , C_2 and C are Σ_1^* , Σ_2^* and Σ^* , respectively.

Whereas the characteristic fluxes φ_k in the machine are associated with the closed curves of the skeleton, the characteristic magnetomotive forces f_k and currents i_k are associated with the curves (not necessarily closed) and the surfaces of the co-skeleton. The names and the positive orientations of the magnetomotive forces f_k 's are chosen according to those of the corresponding fluxes φ_k 's.

The divergence free character of induction, $\text{div } \mathbf{b} = 0$, yields for any volume Ω

$$0 = \int_{\Omega} \text{div } \mathbf{b} \, d\Omega = \int_{\partial\Omega} \mathbf{b} \cdot \mathbf{n} \, d\Omega \quad (21)$$

Applying this to the two volumes of the skeleton gives the topological relations

$$\begin{aligned} \varphi_1 &= \varphi + \varphi_{1\sigma} \\ \varphi_2 &= \varphi - \varphi_{2\sigma} \end{aligned} \quad (22)$$

On the other hand, applying (20) to the three surfaces of the co-skeleton yields

$$\begin{aligned} i_1 &= f_1 + f_{1\sigma} \\ i_2 &= f_2 - f_{2\sigma} \\ f &= f_{1\sigma} - f_{2\sigma} \end{aligned} \quad (23)$$

Equations (22) and (23) are exact topological relations. They can be represented by any of the dual equivalent electric circuits depicted in Figs. 4 and 5.

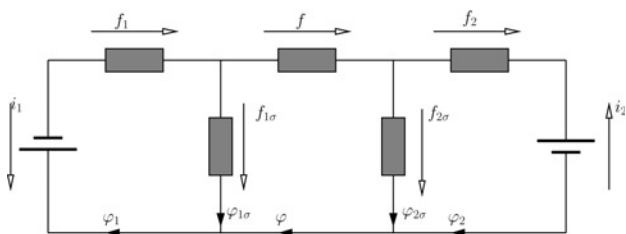


Figure 4 Electric equivalent circuit representing the topological relation (22) in the skeleton and (23) in the co-skeleton

In this circuit, the fluxes φ_k behave like currents, the magnetomotive forces f_k like voltages and the resistances represent the reluctances r_k

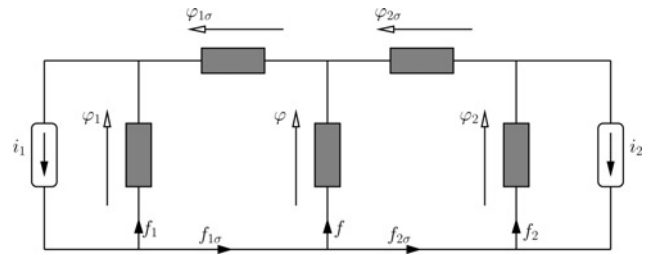


Figure 5 Electric equivalent circuit, dual to the one in Fig. 4

It is associated with exactly the same algebraic relations, but in this case, the fluxes φ_k behave like voltages, the magnetomotive forces f_k like currents and the resistances represent the permeances $(r_k)^{-1}$

6 Constitutive relations

The constitutive relations are relations between dual quantities in the skeleton and the co-skeleton

$$\begin{aligned} f_1 &= r_1 \varphi_1 \\ f_2 &= r_2 \varphi_2 \\ f_{1\sigma} &= r_{1\sigma} \varphi_{1\sigma} \\ f_{2\sigma} &= r_{2\sigma} \varphi_{2\sigma} \\ f &= r \varphi \end{aligned} \quad (24)$$

All the reluctances r_k 's are positive, because of the concordant choice of the positive orientations for the f_k 's and the φ_k 's.

To obtain the classical equivalent circuit of an induction machine in the end, one has now to recognise that the dominant reluctances are that of the air gap and that of the stray flux paths. Consequently, the reluctances r_1 and r_2 are negligible and one can reasonably state that

$$r_1 \simeq 0 \Rightarrow f_1 \simeq 0 \quad (25)$$

$$r_2 \simeq 0 \Rightarrow f_2 \simeq 0 \quad (26)$$

Assuming the fluxes φ_k and the currents i_k are known (see the next section), the remaining reluctances are evaluated as follows

$$r_{1\sigma} = \frac{i_1}{\varphi_1 - \varphi} \quad (27)$$

$$r_{2\sigma} = \frac{-i_2}{\varphi - \varphi_2} \quad (28)$$

$$r = \frac{i_1 + i_2}{\varphi} \quad (29)$$

They are all positive, since $i_2 \leq 0$. This can be written under matrix form as

$$\begin{pmatrix} \varphi_1 \\ \varphi_2 \end{pmatrix} = \begin{pmatrix} \frac{1}{r_{1\sigma}} + \frac{1}{r} & \frac{1}{r} \\ \frac{1}{r} & \frac{1}{r_{2\sigma}} + \frac{1}{r} \end{pmatrix} \begin{pmatrix} i_1 \\ i_2 \end{pmatrix} \quad (30)$$

This matrix is the discrete Hodge operator [12] associated with the discretisation of the system by the skeleton and the co-skeleton.

7 Relation between skeleton quantities and phase quantities

To show how skeleton quantities and phase quantities are related, a practical example is considered. Fig. 1 shows the cross-section of an eight-pole ($p = 4$) induction motor with double layer stator currents. The phase quantities (i.e. related to the stator coils and rotor coils or bars) are defined as follows. Stator phase currents are assumed sinusoidal

$$I_{1K}(t) = I_1 \cos\left(\omega t - K \frac{2\pi}{m} - \alpha_{I_1}\right) \quad (31)$$

$K = 0, \dots, m - 1$, with m being the number of phases. The current density in stator slots is then given by

$$J_{1K} = \frac{I_{1K} Z_N}{A_{N1} P_{SP}} \quad (32)$$

with A_{N1} the area of a half stator slot, Z_N the number of conductors per half slot and P_{SP} the number of coils connected in parallel. Now, Ω_{1K} represents the section of the K th stator phase coil. This is half the total slot surface occupied by the conductors belonging to the phase under consideration (fill factor accounted for in the definition of the current density). One has

$$\Omega_{1K} = \frac{N_1 A_{N1}}{2m} \quad (33)$$

with N_1 the total number of half slots. It follows

$$W_1 I_{1K} = J_{1K} \Omega_{1K} = \frac{I_{1K} Z_N}{A_{N1} P_{SP}} \cdot \frac{N_1 A_{N1}}{2m} \quad (34)$$

which allows to define the number of turns of the stator phase

$$W_1 = \frac{N_1 Z_N}{2m P_{SP}} \quad (35)$$

By (9), the flux embraced by each of the m stator phases of the machine can be written as

$$\phi_{1K}(t) = \frac{l_z}{I_{1K}} \int_{\Omega_{1K}} J_{1K} \mathbf{a} \, d\Omega_{1K} \quad (36)$$

$$= \frac{W_1 l_z}{\Omega_{1K}} \int_{\Omega_{1K}} \mathbf{a} \, d\Omega_{1K} \quad (37)$$

Because of saturation, they are not necessarily sinusoidal in time. One can write for the fundamental harmonic

$$\phi_{1K}(t) = \phi_1 \cos\left(\omega t - K \frac{2\pi}{m} - \alpha_{\phi_1}\right) \quad (38)$$

$K = 0, \dots, m - 1$, thus defining the amplitude ϕ_1 of stator fluxes.

The corresponding quantities associated with the skeleton and the co-skeleton are defined as follows. In 2D, the vector potential writes $\mathbf{a} \equiv a \mathbf{e}_z$, and a surface whose normal lies in the study plane is represented by a curve, the boundary of which is a pair of points with opposite orientations. The integral of \mathbf{a} over such a boundary amounts to evaluating the difference of the potential between those points. Finding the closed curve embracing maximum flux thus, amounts, to finding the maximum and the minimum of the z -component of the \mathbf{a} field computed by means of a transient 2D Finite Element (FE) analysis. At each time step, the fluxes φ_k are evaluated from the FE computation as follows

$$\varphi_1 = (a_{S_{\max}} - a_{S_{\min}}) \cdot l_z \quad (39)$$

$$\varphi_2 = (a_{R_{\max}} - a_{R_{\min}}) \cdot l_z \quad (40)$$

$$\varphi = (a_{G_{\max}} - a_{G_{\min}}) \cdot l_z \quad (41)$$

where l_z is the axial length of the machine, and the subscripts R , S and G denote, respectively, the stator region, the rotor region and the air gap region.

On the other hand, the currents i_1 and i_2 are obtained by applying (20), that is, summing up all currents flowing through the surfaces Σ_1^* and Σ_2^* of the co-skeleton, which are fixed with respect to the rotating field

$$i_k = \int_{\Sigma_k^*} \mathbf{j} \cdot \mathbf{n} \, d\Sigma_k^*, \quad k = 1, 2 \quad (42)$$

It is observed that

$$i_k = i_{k\max} \cos(\alpha_{I_k} - \alpha_{\phi_k}), \quad k = 1, 2 \quad (43)$$

where $\alpha_{\phi_k} - \alpha_{I_k}$ is the phase shift between the flux and the current in the stator coils ($k = 1$) and in the rotor bars ($k = 2$).

After all transient phenomena have vanished out and a stationary operation has been reached, the skeleton fluxes φ_k , the co-skeleton currents i_k and the phase shifts $\alpha_{I_k} - \alpha_{\phi_k}$ will stay nearly constant in time, except for slight fluctuations because of, for example slotting, and which are averaged out in practice, since equivalent circuits are not expected to account for such details. They can all be evaluated from the FE solutions.

The ratio between φ_1 (39) and ϕ_1 is called λ

$$\phi_1 = \lambda \varphi_1 \quad (44)$$

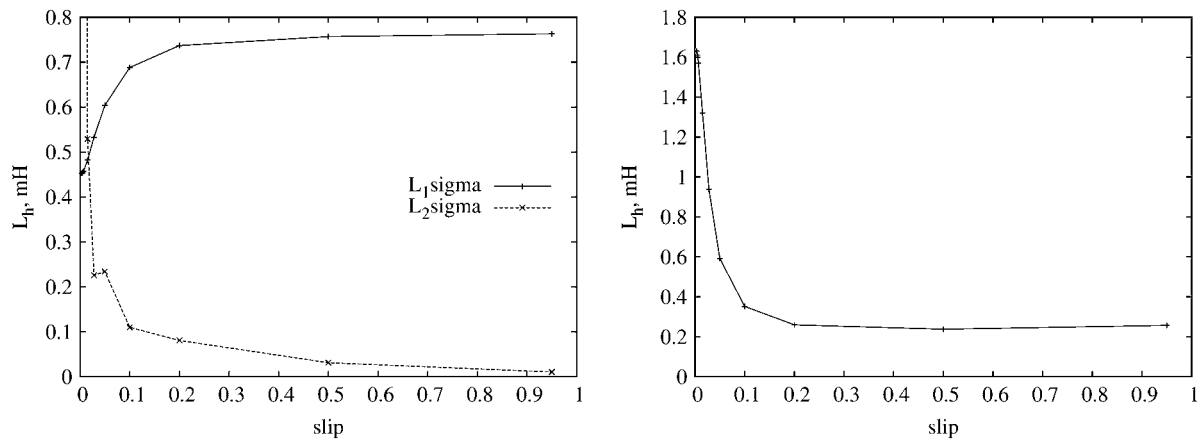


Figure 6 Leakage (left) and magnetising (right) inductances computed at different slips

and the ratio between I_1 and i_{1max} is called κ

$$I_1 = \kappa i_{1max} \tag{45}$$

λ is proportional to the number of turns of the stator coils and to the winding factor, accounting for the spatial distribution of the windings, chording and zoning.

8 Inductance matrix

We can now write

$$\begin{pmatrix} \phi_1 \\ \phi'_2 \end{pmatrix} = \lambda \begin{pmatrix} \varphi_1 \\ \varphi_2 \end{pmatrix} \tag{46}$$

$$\begin{pmatrix} i_1 \\ i_2 \end{pmatrix} = \begin{pmatrix} i_{1max} \cos(\alpha_{I_1} - \alpha_{\phi_1}) \\ i_{2max} \cos(\alpha_{I_2} - \alpha_{\phi_2}) \end{pmatrix} = \frac{1}{\kappa} \Re \left\{ \begin{matrix} I_1 e^{j\alpha_{I_1}} e^{-j\alpha_{\phi_1}} \\ I_2 e^{j\alpha_{I_2}} e^{-j\alpha_{\phi_2}} \end{matrix} \right\} \tag{47}$$

so that the flux-current relation in phasors can be written as

$$\begin{pmatrix} \phi_1 e^{j\alpha_{\phi_1}} \\ \phi_2 e^{j\alpha_{\phi_2}} \end{pmatrix} = \frac{\lambda}{\kappa} \begin{pmatrix} \frac{1}{r_{1\sigma}} + \frac{1}{r} & \frac{1}{r} \\ \frac{1}{r} & \frac{1}{r_{2\sigma}} + \frac{1}{r} \end{pmatrix} \begin{pmatrix} I_1 e^{j\alpha_{I_1}} \\ I_2 e^{j\alpha_{I_2}} \end{pmatrix} \tag{48}$$

We now have the identification

$$L_b = \frac{\lambda}{\kappa} \frac{1}{r} \tag{49}$$

$$L_{1\sigma} = \frac{\lambda}{\kappa} \frac{1}{r_{1\sigma}} \tag{50}$$

$$L'_{2\sigma} = \frac{\lambda}{\kappa} \frac{1}{r_{2\sigma}} \tag{51}$$

and the equation

$$\begin{pmatrix} \phi_1 e^{j\alpha_{\phi_1}} \\ \phi_2 e^{j\alpha_{\phi_2}} \end{pmatrix} = \begin{pmatrix} L_{1\sigma} + L_b & L_b \\ L_b & L'_{2\sigma} + L_b \end{pmatrix} \begin{pmatrix} I_1 e^{j\alpha_{I_1}} \\ I_2 e^{j\alpha_{I_2}} \end{pmatrix} \tag{52}$$

allows defining the lumped inductances of the equivalent T-circuit.

9 Results

Fig. 6 shows leakage and magnetising inductances computed at different slips. The main objective of this paper is to show that the lumped parameters extracted from the field model of the induction motor depend considerably on the working point, especially at small slips where the machine is usually operated. This has been shown here by varying the slip over the range $[0,1[$ with constant stator currents. The determination of the rotor stray inductance $L_{2\sigma}$ is ill-conditioned by this approach because, in (28), one has nearly always $\varphi \simeq \varphi_2$ and $i_2 \simeq 0$. Another evaluation method based on the torque is under investigation. Further work will consist in analysing the relation between the calculated lumped parameters and the different global variables describing the system, in order to obtain a nonlinear equivalent circuit diagram.

10 Conclusion

We have made the distinction between two definitions of fluxes. Thanks to this distinction, one can clearly separate the global (integral) quantities associated with stator phases and rotor coils (or bars) from those associated with the rotating field, and which are carried by a topological structure that we have called the skeleton of the vector potential field. The skeleton, and its topological dual, the co-skeleton, introduce another set of global quantities which can be systematically related to those associated with the stator coils. It makes it possible to deal with fluxes not associated with coils, that is, air gap fluxes and stray fluxes. The lumped parameters obtained by the proposed method turn out not to be constant, whereas most empirical approaches assume they are. They can be systematically extracted from FE simulations of the machine and they deliver a reduced-order model of the induction motor.

11 References

- [1] DAVEY K.R.: 'The equivalent T circuit of the induction motor: its non - uniqueness and use to the magnetic field analyst', *IEEE Trans. Magn.*, 2007, **43**, (4), pp. 1745–48
- [2] DOLINAR D., DE WEERDT R., BELMANS R., FREEMAN E.M.: 'Calculation of 2-axis induction motor model parameters using finite elements', *IEEE Trans. Energy Convers.*, 1997, **12**, (2), pp. 133–142
- [3] FAIZ J., SHARIFIAN M.B.B., FEYZI M.R., SHAARBAFI K.: 'A complete lumped equivalent circuit of 3-phase squirrel-cage induction motors using 2D finite-element techniques', *IEEE Trans. Energy Convers.*, 2002, **17**, (3), pp. 363–367
- [4] KIM D., JUNG H., HAHN S.: 'Equivalent circuit modelling for transient analysis of induction motors with three dimensional finite element analysis'. Proc. IEEE-IEMDC'99, 1999, vol. 201
- [5] NERG J., PYRHÖNEN J., PARTANEN J.: 'Finite element modeling of the magnetizing inductance of an induction motor as a function of torque', *IEEE Trans. Magn.*, 2004, **40**, (4), pp. 2047–49
- [6] WILLIAMSON S., ROBINSON M.J.: 'Calculation of cage induction motor equivalent circuit parameters using finite elements', *IEE Proc. B*, 1991, **138**, (5), pp. 264–276
- [7] YAMAZAKI K.: 'An efficient procedure to calculate equivalent circuit parameter of induction motor using 3D nonlinear time-stepping finite-element method', *IEEE Trans. Magn.*, 2002, **38**, (2), pp. 1281–1284
- [8] SUURINIEMI S., KANGAS J., KETTUNEN L., TARHASAARI T.: 'State variables for coupled circuit problems', *IEEE Trans. Magn.*, 2004, **40**, (2), pp. 949–952
- [9] HENROTTE F., HAMEYER K.: 'The structure of EM energy flows in continuous media', *IEEE Trans. Magn.*, 2006, **42**, (4), pp. 903–906
- [10] LEVA S., MORANDO A.P.: 'Topological transition from magnetic networks to the electric equivalent ones when iron losses are present'. Proc. IEEE Midwest Symp. on Circuits and Systems, Lansing MI, 8–11 August 2000
- [11] CHERRY E.C.: 'The duality between interlinked electric and magnetic circuits and the formation of transformer equivalent circuits'. Proc. Phys. Soc. of London (B), 1949, vol. 2, pp. 101–111
- [12] TARHASAARI T., KETTUNEN L., BOSSAVITA.: 'Some realizations of a discrete Hodge operator: a interpretation of finite element techniques', *IEEE Trans. Magn.*, 1999, **35**, (3), pp. 1491–1497